Printed Circuit Board Reaction Wheels for Small Satellites

Saral Tayal, Paulo Fisch
Carnegie Mellon University
saraltayal@outlook.com,
pfisch@andrew.cmu.edu

Faculty Advisor: Zachary Manchester
Carnegie Mellon University
zacm@cmu.edu

ABSTRACT

Reaction wheels are critical for spacecraft attitude control, enabling precise pointing. However, conventional designs are bulky and expensive, limiting their application in CubeSats and PocketQubes. This paper introduces a novel PCB motor architecture specifically designed for reaction wheels in small satellites. Our design integrates motor windings as traces on the PCB and utilizes a dual-purpose rotor-flywheel combination, resulting in a volumetrically efficient configuration. Additionally, the reaction wheel's PCB casing enables multifunctional capabilities, such as serving as the satellite's structural elements or solar panels. The accessibility of PCB manufacturing offers a simplified and cost-effective production process, with each reaction wheel costing under $100, significantly reducing the cost compared to current commercial-off-the-shelf (COTS) options. Our prototype demonstrates a stall torque of 8 mNm, a maximum power consumption of 5W, and a maximum angular velocity of 170 rad/s, all within a mass of 140g and a thickness of 9mm, facilitating easy integration into a 1U CubeSat. Numerical simulations based on experimental data further validate the performance of our design.

INTRODUCTION

The miniaturization of satellite technology has fueled the widespread use of CubeSats and PocketQubes. However, these miniaturized spacecrafts face significant challenges in achieving effective attitude control. Traditional reaction wheels, designed for larger satellites, are often too large, heavy, and expensive for CubeSats, hindering precise pointing and orientation maneuvers crucial for mission success.1.16. Although magnetorquers offer some integration advantages, their lack of rapid pointing capabilities limits their effectiveness for CubeSats.2. This paper proposes a novel solution to this critical need: a PCB motor architecture specifically designed for reaction wheels in small satellites.

Our approach involves embedding motor windings as PCB traces and using permanent magnets for the rotor. The design uniquely utilizes the PCBs both as the casing and stator, and the rotor as a dual-purpose flywheel. These innovations reduce the mass, cost, and volume of the reaction wheel and offer seamless integration into a CubeSat by allowing the reaction wheel PCB to serve as the outer structure of the satellite, housing various sensors and solar panels.

We detail the development and testing of our prototype, which achieves a stall torque of 8 mNm, a maximum power consumption of 5W, top speed of 170 rad/s, all within a 9mm thick compact design. Numerical simulations based on experimental data validate the performance of our design, demonstrating its viability for small satellite missions. By offering a cost-effective and efficient alternative to existing COTS options, our PCB motor architecture represents a significant advancement in small satellite attitude control technology.

BACKGROUND

Motors are essential for spacecraft, particularly in attitude control systems. Reaction wheels consist of a motor-driven flywheel and are widely used to adjust a spacecraft's orientation by generating reactive torque.10. This precise, continuous control is critical for missions requiring high accuracy, such as Earth imagery and maintaining communication links. Reaction wheels operate based on the principle of conservation of angular momentum: accelerating or decelerating the wheel changes the spacecraft's angular

momentum, allowing for fine pointing adjustments. The dynamics of a reaction wheel-actuated satellite is (1).

$$\frac{dh}{dt} = h \times J \cdot (h - \rho) \quad (1)$$

Where ***h*** is the angular momentum, ***J*** the inertia matrix of the satellite and ρ the angular momentum control input generated by the reaction wheel.

State of the art reaction wheels like those from RocketLab capable of producing 0.01Nm cost upwards of USD 20,000, are bulky at 30mm thick, utilize wire-wound motors, require a mass-inefficient external chassis, and require specialized ball-bearings.15. These drawbacks pose cost and integration complexity for small satellite systems.

DESIGN ARCHITECTURE

Mechanical Arrangement

The Axial Flux motor is assembled in three layers. The first layer (Figure 1) consists of the lower PCB stator, the lower PTFE bushing, and the electronics (MCU, sensors, motor driver). The second layer (Figure 2) consists of the Rotor/Flywheel, the upper PTFE bushing, and the steel axle linking the PCB to the rotors. The third layer (Figure 3) is the upper PCB stator, with bolts holding the entire assembly together.

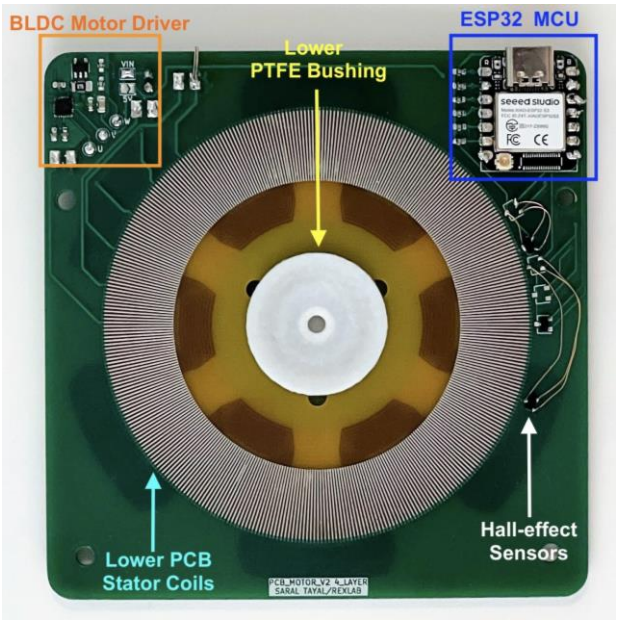

Figure 1: Lower PCB Assembly

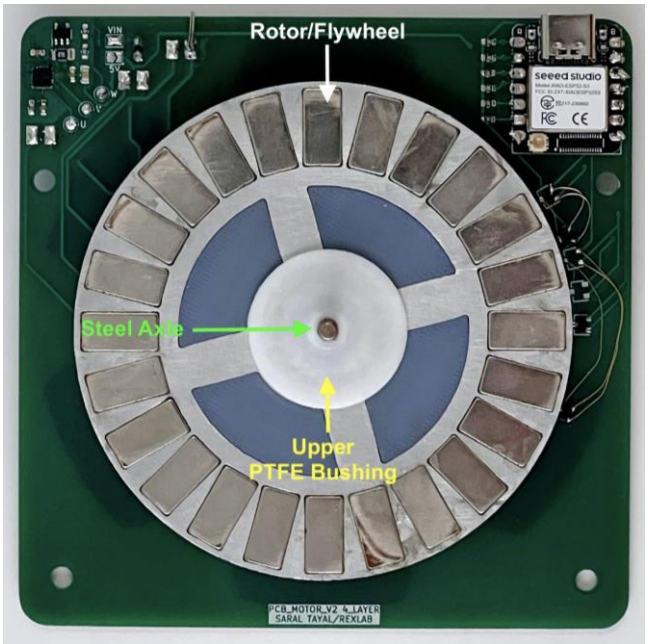

Figure 2: Flywheel stacked on lower PCB

Figure 3: Upper PCB Assembly

Both the upper and lower casings of the PCB motors serve as the stator of the motor. This approach maximizes volumetric efficiency in several ways. Firstly, it creates a more efficient stator with coils in parallel to reduce coil resistance. Secondly, it maximizes torque by engaging both sides of the magnetic field of the permanent-magnet rotor. Thirdly, it enables the use of thinner bushings since the rotor is constrained by two sides of the casing, bringing the rotor closer to the stator, further increasing torque.

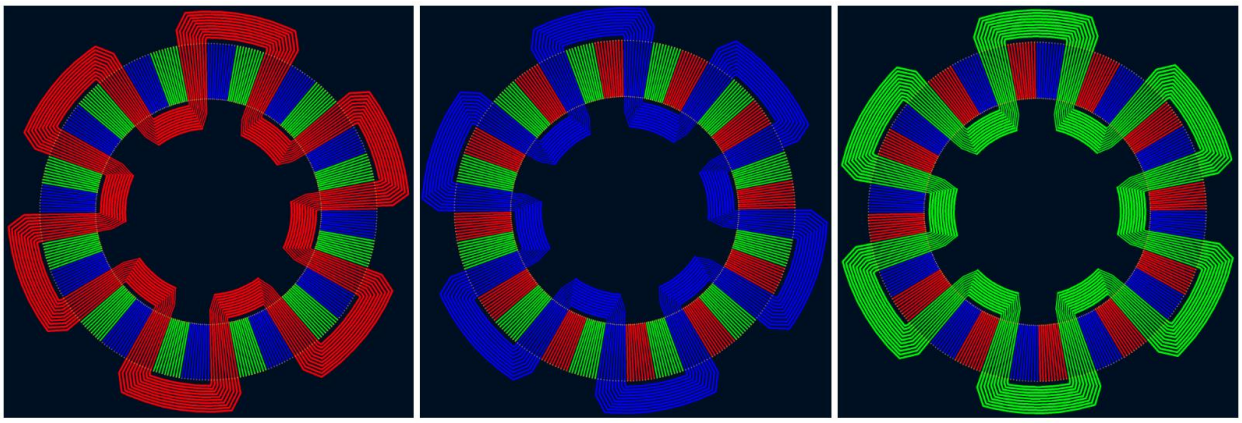

PCB Layer 1 PCB Layer 2 PCB Layer 3

Figure 5: 3 layers of the PCB motor, each layer connecting one phase (Blue: Phase A, Green: Phase B, Red: Phase C)

Winding patterns / Configurations

Traditional copper-wound BLDC motors allow overlapping windings due to enamel-coated windings; PCB coil windings do not offer this flexibility. This poses the challenge of maximizing surface area utilization while routing the start and end of a coil.

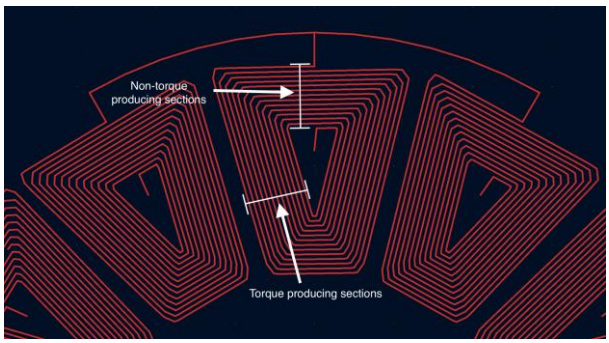

Figure 4: Flywheel stacked on lower PCB

The conventional PCB coil approach involves tracing a coil from inside to outside and vice versa in a 'spiral winding' across various layers, limiting design flexibility and increasing coil resistance.7. Traditional spiral winding designs also suffer from 'dead copper' – sections of the winding that do not generate rotational force (Figure 4), posing a challenge in making an efficient PCB motor for a power-constrained system.7.

Wave-winding coil techniques can offer more efficient PCB motors.5.6.8.9. We designed our own winding-pattern that unwraps a traditional coil and loops it around the entire stator, ensuring that only the torque-producing sections of the coil are positioned underneath the rotor, maximizing torque generation. This design also allows perfect alignment of each section of the coil perpendicular to the rotor's magnetic field, increasing efficiency.

To reduce coil resistance, we optimized by spreading each phase's connections to different layers: Phase A on layer 1, Phase B on layer 2, and Phase C on layer 3 (Figure 5). This separation granted extra space for thicker trace widths and better spread of coil connections. Each torque-producing section of the coil was stitched in parallel to run across all layers in the PCB, further reducing coil resistance (Figure 7).

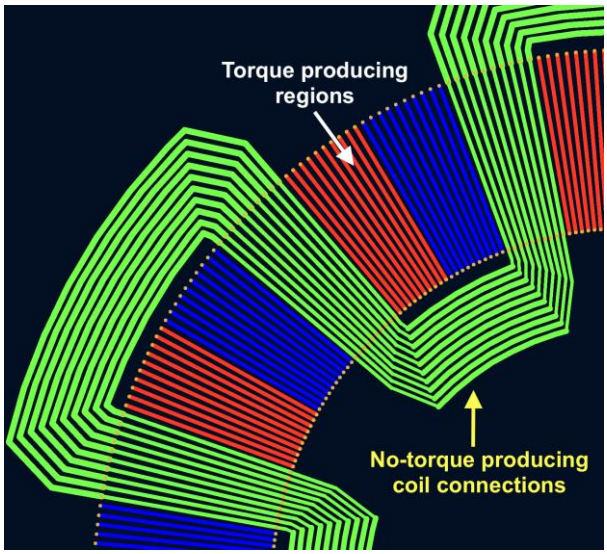

Figure 6: Wave-Winding phases

This winding technique requires a minimum of a three-layer PCB but can scale to any number of layers, where

each additional layer reduces coil resistance, increasing efficiency. This design allows easy integration into a satellite, where inner layers of the satellite's structural PCB serve as the stator for the motor, and the outer layer serves as the solar panel and sensor layer.

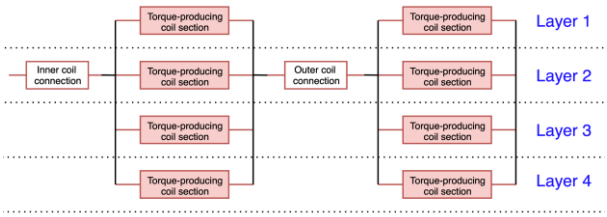

Figure 7: Block diagram of Phase B's coil

These wave-windings are procedurally generated based on input parameters such as coil diameter, pole pairs, and coil turns. The output from our Python script.3 can be directly input into KiCAD.11, enabling anyone to make their own PCB motors.

Cored motors

Traditional wire-wound motors can add a core (often iron) to each coil, increasing torque and efficiency at the cost of top speed, impulse response, and cogging torque.4. Adding a core to a PCB motor is a challenging packaging problem. We experimented with adding a 'copper pour' to each phase on layer 4, which provided no measurable performance gains. Further prototyping with a cored design could yield improved performance.

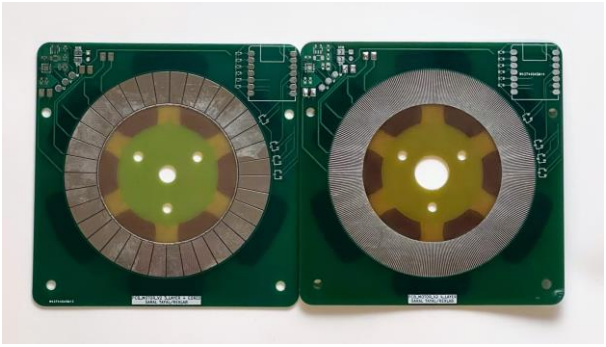

Figure 8: Prototype Core and Coreless design

Bearings vs bushings

Minimizing the stator-to-rotor air gap is crucial for making the motor as efficient and slim as possible. Traditional bearings present challenges in lubrication and wear in space and pose an integration challenge that increases the reaction wheel's thickness by 30-50%.

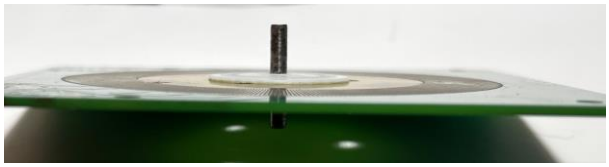

Figure 9: Axle and PTFE bushing on lower PCB stator

We experimented with machining PTFE stock on a lathe to create a custom bushing. The axle rides on the central bore of the bushing, and the outer flange keys the bearing into the PCB (Figure 9) and prevents the rotor from crashing into the PCBs. Benchmarking these bushings, the motor draws 9% more power than equivalently sized ball bearings.

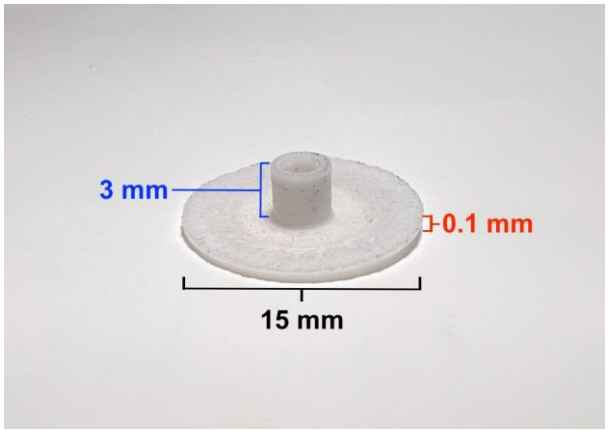

Figure 10: Machined PTFE bushing

Benchmarking these bushings, the motor draws 9% more power than equivalently sized ball bearings.

Magnets & Rotor Design

We selected 0.5" x 0.25" x 0.125" N42 NdFeB magnets arranged in a 12 pole-pair configuration. Purpose-built arc-segment magnets could offer better space utilization but are difficult to source off-the-shelf in the exact desired size.

The rotor is constructed with a waterjet 3mm aluminum sheet and a 3D-printed inner carrier (Figure 2). Prototyping revealed that heat and magnetic forces would warp an exclusively 3D-printed rotor, necessitating the stiffer aluminum frame.

Control Electronics & Firmware

We used hall effect sensors to sense rotor position. Optical encoders could offer a better off-axis sensing solution but were not explored in this effort.

The BLDC motor is controlled by an ESP32S3 and TMC6200 running SimpleFOC.13. The ESP32S3 has two cores, enabling one to run the FOC control loop and the other to handle peripherals such as encoder polling, state machines, and USB communication. Running the FOC control loop as fast as possible is imperative for an efficient and well-performing motor. The TMC6200 offers an efficient 3x3mm BLDC motor control solution without the need for external FETs. All electronic components fit within a 2cm x 2cm footprint between the PCB layers, enabling an all-in-one footprint (Figure 1).

EXPERIMENTAL SETUP

We built a prototype motor with the following parameters.

Configuration	36 Slot, 12 Pole-Pair.12
Dimensions	100mm x 100mm x 9mm
Mass	140g
Flywheel rotational inertia	7.39g/mm²
Max Speed	1600 rpm
Phase resistance	5.5 Ohms
Peak torque	8 mNm

This PCB motor architecture was benchmarked using an inertia dynamometer. An external AS5048A magnetic encoder measured angular positions and velocities with higher precision than the motor's hall-effect sensors. We commanded 100% torque and captured the velocities and acceleration over time, allowing us to back-calculate system torque using T=I×A.

These experiments were conducted at a supply voltage of 8V. The motor can produce additional torque at higher voltage; however, the TMC6200 faced stability issues at higher voltages.

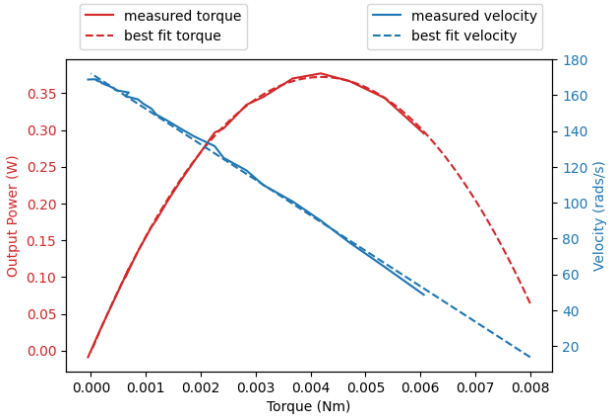

Figure 11: Motor's torque-speed-power curve

NUMERICAL SIMULATIONS

We used the reaction wheel properties detailed in the previous section to inform numerical simulations of a 1.5U cubesat to induce a flat-spin from a tumbling condition. We used an RK4 integrator implemented in Julia for the simulations. The satellite inertia matrix ***J*** is

$$J = \begin{bmatrix} .0043 & -.0003 & 0.0 \\ -0.003 & 0.0049 & 0.0 \\ 0.0 & 0.0 & 0.0035 \end{bmatrix}$$

The satellite is in a 95° inclination Sun-synchronous orbit at an altitude of 550km. The initial condition is random tumbling at a rate of 10°/s. Figure 12 shows the angular momentum trajectory over three orbits.

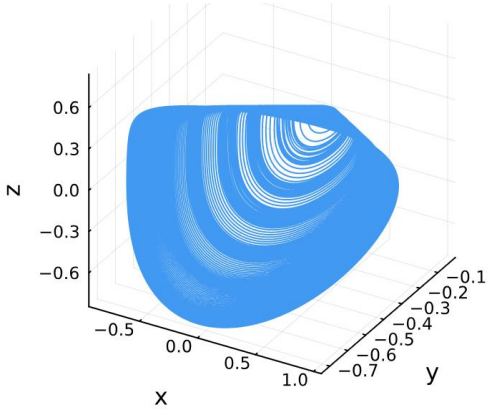

Figure 12: Angular momentum over 3 orbits

Notice the angular momentum converging to the specified major axis of inertia. Therefore, the presented reaction wheels can stabilize the satellite from a tumbling position.

CONCLUSION

In this paper, we presented a novel PCB motor architecture specifically designed for reaction wheels in small satellites. Our design addresses the limitations of conventional reaction wheels by achieving significant reductions in mass, cost, and volume. This is accomplished by leveraging PCBs for both the stator and casing, a hybrid rotor-flywheel design, and unique bushing design. This approach simplifies integration with CubeSats and opens doors for potential applications such as structural elements or solar panels.

Our prototype demonstrates competitive performance metrics, achieving a stall torque of 8 mNm, a maximum power consumption of 5W, and a maximum angular velocity of 170 rad/s all within a 9mm thick design. This, combined with the low mass and cost-effective PCB manufacturing process, makes our design a compelling alternative to existing commercial-off-the-shelf (COTS) options for small satellite attitude control.

Our research suggests promising avenues for further exploration to improve this design:

- **Cored Motor Design**: Investigate the feasibility of incorporating cores into the PCB windings to potentially enhance torque and efficiency.
- **Encoder Integration**: Explore higher precision encoders, such as optical encoders, for improved sensing and motor control.
- **Bushing Material Optimization**: Experiment with alternative bushing materials to achieve a balance between efficiency and ease of machining.

We believe that this PCB motor architecture represents a significant advancement in reaction wheel technology for small satellites. The open-source availability of our design and associated tools like the wave-winding script will hopefully foster further innovation and development in this field.

REFERENCES

1. H.C. Polat et al., "Survey Statistical Analysis and Classification of Launched CubeSat Missions with Emphasis on the Attitude Control Method," *Journal of Small Satellites*. Vol. 5, No. 3, 2016. [Online]. Available: http://www.jossonline.com/wp-content/uploads/2016/10/Final-Survey-Statistical-Analysis-and-Classification-of-Launched-CubeSat-Missions-with-Emphasis-on-the-Attitude-Control-Method3.pdf.
2. A. Puzev et al., "Mass-Ejecting Reaction Wheel for CubeSat Small Orbit Corrections," *Journal of Spacecraft and Rockets*, vol. 59, No. 1, 2022. [Online]. Available: https://arc.aiaa.org/doi/full/10.2514/1.A35042.
3. S. Tayal, "PCB Motors," GitHub repository, 2024. [Online]. Available: https://github.com/SaralTayal123/PCB_Motors.
4. Neethu S et al., "Performance Comparison Between PCB-Stator and Laminated Core Stator Based Designs of Axial Flux Permanent Magnet Motors for High-Speed Low-Power Applications ," *IEEE*, vol. 67, no. 7, pp. 5269-5277, July 2020, [Online]. Available: https://ieeexplore.ieee.org/abstract/document/8789683.
5. N. Taran et al., " *WAVED: A Coreless Axial Flux PM Motor for Drive Systems with Constant Power Operation*," IEEE (ITEC), 2019, pp. 1-6, [Online]. Available: https://ieeexplore.ieee.org/abstract/document/8790489.
6. X. Wang et al., "*Winding Design and Analysis for a Disc-Type Permanent-Magnet Synchronous Motor with a PCB Stators*," *Energies*, vol. 11, no. 12, 2018. [Online]. Available: https://www.mdpi.com/1996-1073/11/12/3383.
7. O. Taqavi et al., "*Design aspects, winding arrangements and applications of printed circuit board motors: a comprehensive review* ," *IET Electric Power Applications*, vol. 14, 2020. [Online]. Available: https://ietresearch.onlinelibrary.wiley.com/doi/full/10.1049/iet-epa.2020.0141.
8. P. Sarbajit et al., "*Comparative analysis of wave winding topologies and performance characteristics in ultra-thin printed circuit board axial-flux permanent magnet machine* ," *IET Electric Power Applications*, vol. 13, 2019. [Online]. Available: https://ietresearch.onlinelibrary.wiley.com/doi/10.1049/iet-epa.2018.5417.
9. Tokgöz F et al., "*Comparison of PCB winding topologies for axial-flux permanent magnet synchronous machines*," IET Electric Power Applications, vol. 14, 2020. [Online]. Available: https://ietresearch.onlinelibrary.wiley.com/doi/full/10.1049/iet-epa.2020.0622
10. A. Siahpush, "*A BRIEF SURVEY OF ATTITUDE CONTROL SYSTEMS FOR SMALL*

SATELLITES USING MOMENTUM CONCEPTS," *Small Satellites Conference*, 1988. [Online]. Available: https://digitalcommons.usu.edu/cgi/viewcontent.cgi?article=2394&context=smallsat.
11. Atomic14, "KiCad Coil Plugins," GitHub repository, 2021. [Online]. Available: https://github.com/atomic14/kicad-coil-plugins.
12. Bavaria Direct, "*Electric Motor Calculator*," [Online]. Available: https://www.bavaria-direct.co.za/scheme/calculator/.
13. SimpleFOC Team, "*SimpleFOC: A Simple Field Oriented Control Library*," [Online]. Available: https://www.simplefoc.com/.
14. T. R. Kane, P. W. Likins, D. A. Levinson et al., "*Spacecraft Dynamics*". McGraw-Hill New York, 1983, vol. 1.
15. Rocket Lab USA, "10 mNms Reaction Wheel: Data Sheet," [Online]. Available: https://www.rocketlabusa.com/assets/Uploads/10-mNms-RW-0.01-Data-Sheet.pdf
16. L. He, W. Ma, P. Guo, and T. Sheng, "*Developments of attitude determination and control system of microsats: A survey*," Proceedings of the Institution of Mechanical Engineers, Part I: Journal of Systems and Control Engineering, vol.235, no. 10, pp. 1733–1750, Nov. 2021. [Online] Available:http://journals.sagepub.com/doi/10.1177/0959651819895173